Thermophysical Properties of Quartzite for High Temperature Thermal Storage

January 2021

This Activity received funding from ARENA as part of ARENA's Commercialisation of R&D Funding Initiative Pilot

Project Title: Displacement of Gas by Thermal Energy Storage

Project Number: 2019/CRD004

Recipient: Future Industries Institute, University of South Australia

Contact: Professor Frank Bruno

Phone: (08) 8302 3230

Email: frank.bruno@unisa.edu.au

Authors: Dr. Rhys Jacobs, Prof. Frank Bruno

The University of South Australia
Future Industries Institute | Mawson Lakes Campus
Mawson Lakes | SA 5095 | AUSTRALIA

Executive Summary

The thermophysical properties of a filler material (quartzite), which will be utilised for high temperature thermal energy storage, have been determined. The characterised material will be utilised as the storage media in an electrically-charged, air-based packed-bed system, which will be demonstrated at UniSA. Equations for the specific heat, density and porosity of the material have been determined. The quartzite, which is readily commercially available and inexpensive, was found to have sufficient durability for this purpose, based on the results of thermal cycling tests and associate macrostructural and microstructural analyses.

Table of Contents

Executive Summary ..... **ii**

1 Introduction **1**

1.1 Objective 1

1.2 Background 1

2 Materials **3**

3 Methodology **3**

3.1 Specific Heat 3

3.2 Density and Porosity Measurements 3

3.3 Microstructure Analysis Using Scanning Electron Microscopy and Energy Dispersive X-Ray Spectroscopy (SEM/EDS) 4

4 Results and Discussion **5**

4.1 Measured Specific Heat 5

4.2 Impact of Thermal Cycling 6

4.2.1 Macroscopic Appearance 6

4.2.2 Weight Loss 7

4.2.3 Impact on Specific Heat 8

5 Conclusions **10**

6 References **11**

List of Figures

Figure 1- Quartzite Samples Prior to Thermal Cycling 3
Figure 2- Measured Quartzite Heat Capacity 5
Figure 3- Uncycled (Top) and 50 Cycled (Bottom) Samples 6
Figure 4- Uncycled (Top) and 100 Cycled (Bottom) Samples 6
Figure 5- Uncycled (Top) and 200 Cycled (Bottom) Samples 6
Figure 6- Measured Specific Heat after 50 Thermal Cycles 8
Figure 7- Measured Specific Heat after 100 Thermal Cycles 8
Figure 8- Measured Specific Heat after 200 Thermal Cycles 8
Figure 9- Comparison of Uncycled and Thermally Cycled Quartzite 9

List of Tables

Table 1- Desirable Properties of Storage Media 1
Table 2- Thermo-physical Properties of Quartzite Rock 1
Table 3- Comparison of Sensible Materials for High Temperature Thermal Storage 2
Table 4- Measured Sample Weights Before and After Cycling 7

1 Introduction

1.1 Objective

To experimentally verify the thermophysical properties of a filler material (quartzite) that can be utilised for high temperature thermal storage. The characterised material is intended to be utilised as the storage media in an electrically-charged, air-based packed bed system to be demonstrated at UniSA.

1.2 Background

Quartzite is the name given to nonfoliated metamorphic rock composed almost entirely of quartz (SiO_2). It forms when a quartz-rich sandstone is altered by the heat, pressure, and chemical activity of metamorphism. These conditions recrystallize the sand grains and the silica cement that binds them together. The result is a network of interlocking quartz grains of incredible strength. The interlocking crystalline structure of quartzite makes it a hard, tough, durable rock. It is normally white and/or grey in colour but can have pink, red, purple staining due to the presence of iron (King 2020).

In regards to high temperature thermal storage, Khare et al. (2013) describe that materials should meet five key criteria *(Table 1)*.

Table 1- Desirable Properties of Storage Media

Property	Desirable Characteristic(s)
Thermo-physical	High energy density (per unit mass or volume), high thermal conductivity, high heat capacity, high density, long term thermal cycling stability
Chemical	Long term chemical stability with no chemical decomposition, non-toxic, non-explosive, low corrosion potential or reactivity to HTFs, and compatible with materials of construction
Economic	Cheap and abundant materials with low cost of manufacturing into suitable shapes
Mechanical	Good mechanical stability, low coefficient of thermal expansion, high fracture toughness, high compressive strength
Environmental	Low manufacturing energy requirement and CO_2 footprint

When compared against the above criteria, quartzite rock performs favourably. Quartzite rock has a relatively high density, high thermal conductivity, and relatively high heat capacity as shown in *Table 2* (Xu et al., 2012).

Table 2- Thermo-physical Properties of Quartzite Rock

Property	Value
Density	2,500 kg/m^3
Thermal Conductivity	5.69 W/mK
Specific Heat Capacity	0.83 J/gK

Because of its desirable thermo-physical properties, it has been suggested as a storage material in packed bed thermoclines previously (Pacheco et al., 2002, Brosseau et al., 2004, EPRI, 2010). When tested with solar salt (60 wt% $NaNO_3$: 40 wt% KNO_3) the quartzite samples did not show signs of degradation and chemical incompatibility (Pacheco et al., 2002, Brosseau et al., 2004). Other air-based systems have previously proposed and/or utilised quartzite (or a blend) material with success, especially when coupled with phase change materials (PCMs) (Zhao B-C et al., 2016; Zanganeh et al., 2014, 2015; Galione et al., 2015; Geissbühler et al., 2018; Jacob et al., 2019).

This is in contrast to experimental data from Soprani et al. (2019) who suggest that quartzite is not a suitable material at high temperatures due to the 'interstitial phases' which break down at temperature, weakening the rock. While the crystal inversion from α-quartz to β-quartz at 573°C is well studied, the repeated thermal cycling and stress due to linear expansion (0.45 %) impact on the stability of the material is yet to be determined.

The cost of the media has been estimated to cost between $_{US}0.02-0.043/kg (Pacheco et al., 2002; Galione et al., 2015) while recent quotes for the current storage system are around $_{AU}0.072/kg. As it is a mined and naturally occurring product, it does not require further manufacturing (only crushing), while the environmental impact is also low.

Finally, a comparison to other sensible storage materials is shown in *Table 3*.

Table 3- Comparison of Sensible Materials for High Temperature Thermal Storage

Material	Density (kg/m^3)	Heat Capacity (kJ/kg·K)	Cost (USD/kg) ^	Energy Density (kJ/m^3)*	Cost of Energy Density (kJ/USD)*	REF
AAM [Fly ash/Black Slag]	2,592	1.6	0.07	1,119,744	6,171	*Jacob et al. (2020)*
Alumina	3,953	1.16	0.35	1,238,080	895	Ortega-Fernandez et al. (2015)
Rock/Quartz	2,500	0.83	0.2	560,250	1,121	Galione et al. (2015)
Silicon Carbide	3,210	0.75	1.03	650,025	197	Jacob et al. (2016)
Castable Ceramic	3,500	1.35	5	1,275,750	73	Ortega-Fernandez et al. (2015)
Cofalit®	3,120	0.86	0.01	724,464	23,220	Ortega-Fernandez et al. (2015)
EAF Slag 1	3,430	0.93	0.09	861,273	2,790	Ortega-Fernandez et al. (2015)
EAF Slag 2	3,770	0.91	0.09	926,289	2,730	Ortega-Fernandez et al. (2015)
Solar Salt	1,870	1.6	0.69	807,840	626	Ortega-Fernandez et al. (2015)
WBA	2,586	0.29	0.0006	202,473	130,500	del Valle-Zermeño et al. (2016)
Magnetite	5,150	1.1	0.18	1,529,550	1,650	Grosu et al. (2017)

**Based on a ΔT=270°C*

^ Costs indicated are for raw material only. Does not include any further processing etc. that may be required.

From *Table 3* it can be seen that while quartzite compares favourably with other materials such as alumina, magnetite, and silicon carbide, it may represent a slightly costlier material than other waste

based materials such as EAF Slag, WBA, and AAMs. However, given that these materials need further processing and are not produced in large enough quantities for commercial systems, quartzite rock represents a simple and cost-effective choice for the current project. Furthermore, should an alternative storage material prove more cost-effective and available, there is always the potential to alter storage materials while maintaining the same storage design.

2 Materials

The quartzite rocks (to act as the filler material) tested in the current study were obtained locally from Garden Grove Supplies[1]. The samples were random in shape but nominally were 20 mm in size (see *Figure 1*) as suggested as the most cost effective size for packed bed systems (Jacob et al., 2019).

Figure 1- Quartzite Samples Prior to Thermal Cycling

Samples were chosen at random to be tested for the relevant thermal and physical properties.

3 Methodology

The experimental procedure to determine important thermal and physical parameters are described below. The tested properties include specific heat, thermal stability, and density. Furthermore, samples were chemically and physically characterised using scanning electron microscopy (SEM) and xray diffraction (XRD).

3.1 Specific Heat

The thermophysical property of heat capacity was measured using a direct scanning calorimeter (404-F1 Jupiter, Netzsch) (DSC). Five samples were taken from several samples of the material as a powder between 20-40 mg and placed in 0.3 mL graphite crucibles. To measure the heat capacity, the sample is subject to a heating cycle under nitrogen flow (20 ml/min). The sample is held isothermally for 10 minutes at the desired start temperature (100°C) before being heated to 800°C at a rate of 10°C/min. The sample is then held at this temperature for 10 minutes before being cooled. To determine the heat capacity, the material was compared to a known reference (sapphire) according to the procedure outlined in ASTM E 1269.

3.2 Density and Porosity Measurements

The density and porosity of samples was measured using the Archimedes principle *(Equation [1])* using water as the fluid.

[1] https://gardengrove.com.au/product/20mm-quartz-metal/

$$\rho_{Qz} = \rho_{H_2O} * \frac{W_{Qz}}{W_{H_2O\ displaced}} \quad \textbf{[1]}$$

Where ρ is the density of the quartzite material (Qz) and water (H_2O). The weight of the water displaced was estimated by measuring the rise of volume in a graduated measuring cylinder *Equation [2]*.

$$W_{H_2O\ displaced} = \left(V_{H_2O,a} - V_{H_2O,b}\right) * \rho_{H_2O} \quad \textbf{[2]}$$

Where V_{H2O} is the volume before (b) and after (a) the sample is placed in the water.

The porosity measurements were done using dry, saturated, and submerged sample masses *([3])*. The fluid used was RO water.

$$Porosity = \frac{W_{Sat} - W_{Dry}}{W_{Sat} - W_{Sub}} \quad \textbf{[3]}$$

3.3 Microstructure Analysis Using Scanning Electron Microscopy and Energy Dispersive X-Ray Spectroscopy (SEM/EDS)

Samples were analysed using a Zeiss Merlin field emission electron gun SEM and silicon drift detector EDS. Fracture surfaces were used to observe porosity and localized heterogeneity. Samples were then ball milled and re-examined to represent overall composition.

3.4 Thermal Cycling

To determine the cyclic stability of the chosen storage material, samples were thermally cycled between 200°C-700°C. Samples were then removed after 50, 100, and 200 cycles and compared to the properties of uncycled materials. To produce a representative sample, sub-samples were taken randomly from three of the six samples, crushed, and mixed.

4 Results and Discussion

The following section describes the experimental results and their implications.

4.1 Measured Specific Heat

The specific heat of the material was determined by using the average values of three out of five samples tested. These samples were chosen to minimise the impact of random errors that may have occurred. The error (determined by the shaded area) was determined by taking the minimum and maximum measured value at each temperature point. Lastly, during measurement, the data for the specific heat above 700°C became erratic and is therefore excluded from the current study. The measured heat capacity of the uncycled samples is given in *Figure 2*.

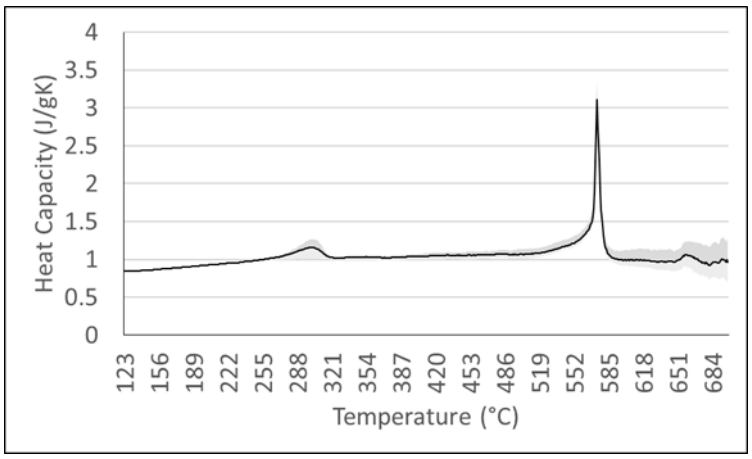

Figure 2- Measured Quartzite Heat Capacity

From *Figure 2*, it can be seen that in general the specific heat marginally rises with temperature. There is a minor peak around 300°C which may be due to the oxidation of metallic elements, while there is a larger peak at 573°C. This peak at 573°C is attributed to the reversible crystal inversion from α-quartz to β-quartz (Lider et al., 2014). Overall the specific heat of the quartzite storage material can be described by *Equations [4] and [5].*

$Cp_{Qz} = 5.500E-4 * T + 0.83$	125-550°C	**[4]**
$Cp_{Qz} = 1.365E-3 * T + 0.28$	600-700°C	**[5]**

4.2 Impact of Thermal Cycling

4.2.1 Macroscopic Appearance

Initially, the quartzite rocks are whitish with brown/silver specks throughout as illustrated in *Figure 1* and the top row in *Figure 3, Figure 4* and *Figure 5*. However, as can be seen by the bottom rows in these same three figures, after thermal cycling the quartzite rocks now appear pinkish or purple in nature.

Figure 3- Uncycled (Top) and 50 Cycled (Bottom) Samples

Figure 4- Uncycled (Top) and 100 Cycled (Bottom) Samples

Figure 5- Uncycled (Top) and 200 Cycled (Bottom) Samples

4.2.2 Weight Loss

In addition to the macroscopic change that has occurred through the samples, the weight of the samples was measured before and after cycling to determine thermal stability. A large weight loss would indicate thermal instability and unsuitability to be used as a high temperature storage material. The measured weights before and after each cycle number for the tested samples are given in *Table 4*.

Table 4- Measured Sample Weights Before and After Cycling

Batch/Cycle	Sample	Uncycled	Cycled	% change	
50	1	5.47	5.46	-0.18%	-0.50%
	2	5.13	5.05	-1.56%	
	3	1.96	1.95	-0.51%	
	4	5.46	5.44	-0.37%	
	5	5.95	5.95	0.00%	
	6	2.8	2.79	-0.36%	
100	1	8.69	8.67	-0.23%	-0.37%
	2	3.76	3.74	-0.53%	
	3	3.95	3.94	-0.25%	
	4	3.15	3.14	-0.32%	
	5	10.52	10.45	-0.67%	
	6	4.34	4.33	-0.23%	
200	1	6.66	6.62	-0.60%	-0.33%
	2	7.91	7.89	-0.25%	
	3	2.06	2.06	0.00%	
	4	8.82	8.81	-0.11%	
	5	7.31	7.27	-0.55%	
	6	8.9	8.86	-0.45%	

As can be seen from *Table 4* there is minimal difference in the measured weight before and after cycling, indicating excellent thermal stability. Across all samples the average weight loss was 0.4 %, while the weight loss at 50 cycles was marginally higher than at 200 cycles. This is most likely to the high weight loss experienced by one of the samples as opposed to an inherent factor.

4.2.3 Impact on Specific Heat

The specific heat of the cycled samples was determined using the same methodology presented in *Section 4.1*. The measured specific heat for 50, 100, and 200 cycles are shown in *Figure 6*, *Figure 7* and *Figure 8*, respectively. Finally, the data from these three figures and the uncycled material are compared in *Figure 9*.

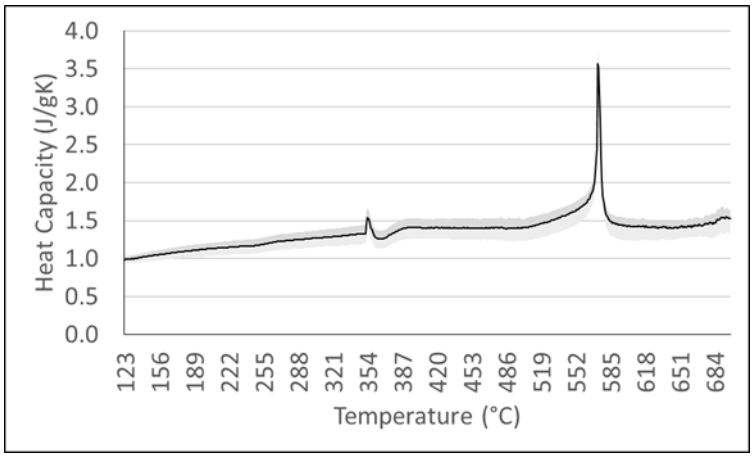

Figure 6- Measured Specific Heat after 50 Thermal Cycles

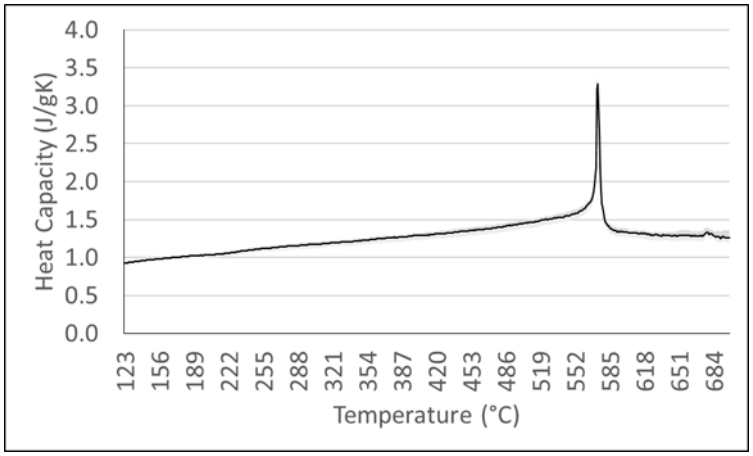

Figure 7- Measured Specific Heat after 100 Thermal Cycles

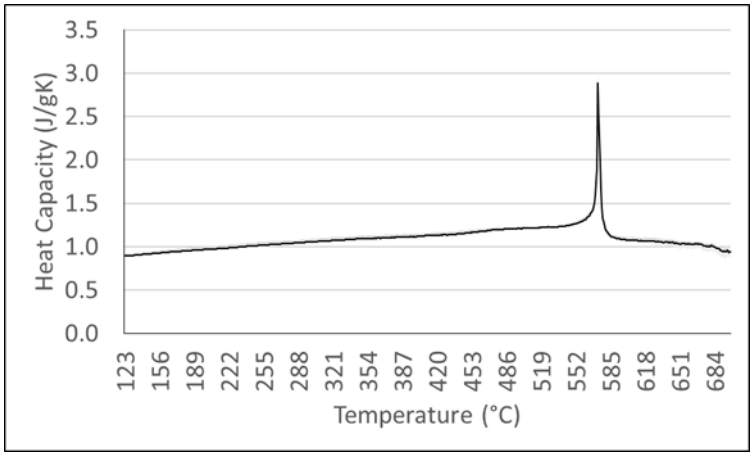

Figure 8- Measured Specific Heat after 200 Thermal Cycles

From *Figure 9* it can be seen that the uncycled sample has a small 'bump' at approximately 300°C, potentially due to the formation of metal oxides. This is more pronounced after 50 cycles; however, the 'bump' has moved to ≈360°C, possibly indicating a secondary reaction. In both the 100 and 200 cycles there is no evidence of reaction/oxide formation, suggesting that this phenomenon is complete by 100 cycles. Furthermore, it would appear that there is an increase in the specific heat of the sample in the early cycles (<200 cycles) before returning to values reminiscent of the uncycled samples. In all samples there is evidence of the α- to β-quartz transition at ≈573°C. Therefore, it is suggested that while there is some change in the quartzite due to thermal cycling, any changes are temporary, and the specific heat of the storage material should be considered as unchanging due to thermal cycling.

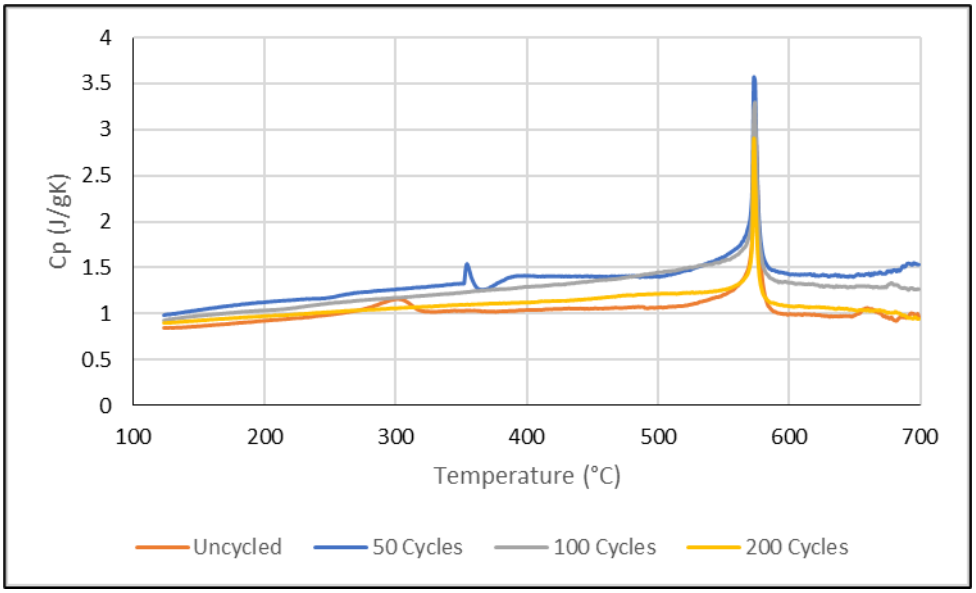

Figure 9- Comparison of Uncycled and Thermally Cycled Quartzite

5 Conclusions

The thermophysical properties of quartzite, including specific heat, density and porosity, have been determined and this material has been deemed suitable for use as the storage media in an electrically-charged, air-based packed-bed system. The quartzite is readily commercially available, inexpensive and has sufficient durability for this purpose, based on the results of thermal cycling tests and associate macrostructural and microstructural analyses.

6 References

Brosseau D, Hlava P, Kelly M (2004). *Testing Thermocline Filler Materials and Molten Salt Heat Transfer Fluids for Thermal Energy Storage Systems Used in Parabolic Trough Solar Power Plants*. SAND2004-3207; Albuquerque, NM.

EPRI (2010). *Solar Thermal Storage Systems: Preliminary Design Study*, Rept. 1019581.

Galione P.A, Pérez-Segarra C.D, Rodríguez I, Oliva A, Rigola J. *Multi-layered solid-PCM thermocline thermal storage concept for CSP plants. Numerical analysis and perspectives*. Applied Energy (2015); **142**: 337–351.

Geissbühler L, Becattini V, Zanganeh G, Zavattoni S, Barbato M, Haselbacher A, Steinfeld A. *Pilot-scale demonstration of advanced adiabatic compressed air energy storage, Part 1: Plant description and tests with sensible thermal-energy storage*. Journal of Energy Storage (2018); **17**: 129-139.

Grosu Y, Faik A, Ortega-Fernández I, D'Aguanno B. *Natural Magnetite for thermal energy storage: Excellent thermophysical properties, reversible latent heat transition and controlled thermal conductivity*. Solar Energy Materials & Solar Cells (2017); **161**: 170–176.

Jacob R, Trout N, Solé A, Clarke S, Inés Fernández A, Luisa F. Cabeza, Saman W, Bruno F (2020). *Novel Geopolymer for use as a Sensible Storage Option in High Temperature Thermal Energy Storage Systems*. API Conference Proceedings- SolarPACES 2019; In Press.

Jacob R, Belusko M, Liu M, Saman W, Bruno F. *Using Renewables Coupled with Thermal Energy Storage to Reduce Natural Gas Consumption in Higher Temperature Commercial/Industrial Applications*. Renewable Energy (2019); **131**: 1035-1046.

Jacob R, Trout N, Raud R, Clarke S, Steinberg T.A, Saman W, Bruno F. *Geopolymer encapsulation of a chloride salt phase change material for high temperature thermal energy storage*. AIP Conference Proceedings **1734**, 050021 (2016); DOI: 10.1063/1.4949119.

Khare S, Dell'Amico M, Knight C, McGarry S. *Selection of materials for high temperature sensible energy storage*. Solar Energy Materials & Solar Cells (2013); **115**: 114–122.

King H (2020). *Quartzite*. Available online: https://geology.com/rocks/quartzite.shtml [Last accessed: 8th July 2020]

Lider MC, Yurtseven H. *α- β Transition in Quartz: Temperature and Pressure Dependence of the Thermodynamic Quantities for β-Quartz and β-Cristobalite as Piezoelectric Materials*. 3D Res (2014) 5:28. DOI 10.1007/s13319-014-0028-1

Ortega-Fernandez I, Calvet N, Gil A, Rodríguez-Aseguinolaza J, Faik A, D'Aguanno B. *Thermophysical characterization of a by-product from the steel industry to be used as a sustainable and low-cost thermal energy storage material*. Energy (2015); **89**: 601-609.

Pacheco J, Showalter S, Kolb W. *Development of a Molten-Salt Thermocline Thermal Storage System for Parabolic Trough Plants*. Journal of Solar Energy Engineering (2002); **124**: 153-159.

Soprani S, Marongiu F, Christensen L, Alm O, Petersen KD, Ulrich T, Engelbrecht K. *Design and testing of a horizontal rock bed for high temperature thermal energy storage*. Applied Emergy (2019); **251**: 113345.

del Valle-Zermeño R, Barreneche C, Cabeza L.F, Formosa J, A. Inés Fernández, Chimenos J. *MSWI bottom ash for thermal energy storage: An innovative and sustainable approach for its reutilization*. Renewable Energy (2016); **99**: 431-436.

Xu C, Wang Z, He Y, Li X, Bai F. *Sensitivity analysis of the numerical study on the thermal performance of a packed-bed molten salt thermocline thermal storage system*. Applied Energy (2012); **92**: 65-75.

Zanganeh G, Khanna R, Walser C, Pedretti A, Haselbacher A, Steinfeld A. *Experimental and numerical investigation of combined sensible–latent heat for thermal energy storage at 575°C and above*. Solar Energy (2015); **114**: 77–90.

Zanganeh G, Commerford M, Haselbacher A, Pedretti A, Steinfeld A. *Stabilization of the outflow temperature of a packed-bed thermal energy storage by combining rocks with phase change materials*. Applied Thermal Engineering (2014); **70**: 316-320.

Zhao B-C, Cheng M-S, Liu C, Dai Z-M. *Thermal performance and cost analysis of a multi-layered solid-PCM thermocline thermal energy storage for CSP tower plants*. Applied Energy (2016); **178**: 784–799.